Aggregation-Induced Emission from Fluorophore-Quencher Dyads with Long-Lived Luminescence

ARTICLE *in* THE JOURNAL OF PHYSICAL CHEMISTRY A · JULY 2015

Impact Factor: 2.69 · DOI: 10.1021/acs.jpca.5b06906 · Source: PubMed

THE JOURNAL OF PHYSICAL CHEMISTRY A

Article

pubs.acs.org/JPCA

Aggregation-Induced Emission from Fluorophore−Quencher Dyads with Long-Lived Luminescence

Biao Chen,[†] Xingxing Sun,[†] Ruffin E. Evans,[‡] Rui Zhou,[†] James N. Demas,[§] Carl O. Trindle,[§] and Guoqing Zhang*[,†]

[†]CAS Key Laboratory of Soft Matter Chemistry, Department of Polymer Science and Engineering, University of Science and Technology of China, Hefei 230026, China

[‡]Department of Physics, Harvard University, Cambridge, Massachusetts 02138, United States

[§]Department of Chemistry, University of Virginia, Charlottesville, Virginia 22903, United States

Supporting Information

ABSTRACT: Aggregation-induced emission (AIE) is an important photophysical phenomenon in molecular materials and has found broad applications in optoelectronics, bioimaging, and chemosensing. Currently, the majority of reported AIE-active molecules are based on either propeller-shaped rotamers or donor−acceptor molecules with strong intramolecular charge-transfer states. Here, we report a new design motif, where a fluorophore is covalently tethered to a quencher, to expand the scope of AIE-active materials. The fluorophore−quencher dyad (FQD) is nonemissive in solutions due to photoinduced electron-transfer quenching but becomes luminescent in the solid state. The intrinsic emission lifetimes are found to be within the microseconds domain at both room and low temperatures. We performed single-crystal X-ray diffraction measurement for each of the FQDs as well as theoretical calculations to account for the possible origin of the long-lived AIE. These FQDs represent a new class of AIE-active molecules with potential applications in organic optoelectronics.

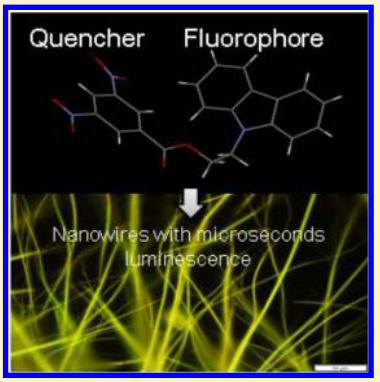

INTRODUCTION

Molecular materials exhibiting aggregation-induced emission (AIE) are very important candidates in various applications such as optoelectronics,[1−8] luminescence chemosensing,[11−15] and biological imaging.[16−23] The advantage of AIE materials arises from their solid-state nature that includes high photoluminescent brightness and low photobleaching rate. These properties are largely due to the suppression of nonradiative pathways such as thermal decays and photochemical reactions, which are more prevalent in the solution state.[6,8−10,24−26] As a result, to be classified as AIE-active molecules, they must be able to dissipate excited-state energies through nonradiative transitions in the solution state whereas in the solid state, such processes must be efficiently shut down to allow for more competitive radiative decays. The first class of AIE-active molecules is based on propeller-shaped "molecular rotamers", which exhibit exceedingly high rotational freedom in solutions.[8] Intramolecular rotations can be sufficiently restricted when aggregation occurs and photoluminescence can be observed. The second class of AIE-active molecules typically involves strong intramolecular charge-transfer (ICT) states, which may adopt a twisted conformation in the excited state in solution.[27−37] Some part of the excited-state potential surface of such twisted conformation may become too close to that of the ground-state one and activates thermal decay very effectively to quench photoluminescence. Inhibition of ICT via molecular aggregation, however, can hinder the twisted excited-state conformation and thus makes the radiative decay more competitive. *Here, we propose a new class of AIE-active materials constructed from organic molecules, where a fluorophore and a quencher are covalently tethered together through a flexible linker*. In solutions, photoinduced electron transfer (PET) leads to the formation of radical ion pairs and entirely quenches the photoluminescence.[38−43] In the solid state, the molecular materials are expected to exhibit some sort of band-like structure and photoluminescence resembling that of organic semiconductors may be obtained under suitable conditions.[44] This prediction is based on the fact that PET normally requires that two organic molecules be paired with a high-energy highest occupied molecular orbital (HOMO) and a low-lying lowest unoccupied molecular orbital (LUMO).[45] The HOMO/LUMO interactions in the solid state in a periodical fashion typically results in excitonic splitting and increased electronic delocalization; the radiative recombination of the delocalized exciton can thus generate luminescence. The binary solid, often a mixture of two organic molecules, is referred to as a "charge-transfer complex (CTC)".[44] There have been a handful of precedents where photoluminescence was observed for CTCs at room temperature (e.g., in crystals[46] and polymers[47]). However, emission from tethered crystalline systems has not

Received: July 17, 2015
Revised: July 27, 2015

DOI: 10.1021/acs.jpca.5b06906
J. Phys. Chem. A XXXX, XXX, XXX−XXX

been reported yet.[48] An obvious advantage of using tethered system is that not only stoichiometry can be guaranteed but also problems such as phase separation can be avoided.

In this article, we report the construction of an AIE system where nitrobenzoates are covalently attached to carbazole (CZ) through an alkyl linker (Chart 1). Five fluorophore−quencher dyads (FQDs) of different linker lengths were synthesized and studied both in solutions and in the solid state. We found that the photoluminescence from these FQDs is entirely quenched in solutions; in the solid state, however, the photoluminescence with long intrinsic lifetimes (1.26−17.9 μs) could be observed. To better understand the origin of the FQD-based AIE system, theoretical calculations for FQD clusters were performed. It was found that calculations with structures drawn from single-crystal X-ray diffraction (XRD) data produce nearly degenerate intermolecular singlet and triplet CT excitations. It can thus be inferred that the long-lived emission has significant involvement of the triplet state. We also found that these FQDs spontaneously form nanowire or nanosheet structures in solution-cast samples, observed by fluorescence and transmission electron microscopies. These FQDs represent a new class of AIE-active molecules with potential applications in organic optoelectronics.

Chart 1. Chemical Structures of Fluorophore−Quencher Dyads (FQDs)

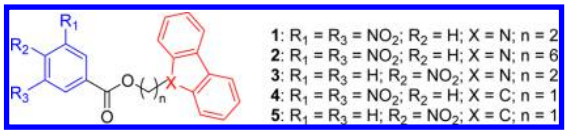

RESULTS AND DISCUSSION

The fluorophores of these FQDs are modified by the linking atom (X = N for **1**−**3** or X = C for **4**−**5**) and quenchers vary in the number and position of nitro groups on the benzene ring with three types of alkyl linkers. All of the FQDs are nonemissive in solution and barely show intramolecular interactions from UV−vis spectroscopy (see Supporting Information, for spectra and more discussion). In comparison, the yellow and orange crystalline solids of **1**−**3** are significantly luminescent to the naked eye under a UV lamp (λ_{ex} = 365 nm); no noticeable emission was observed for the colorless crystal **4** and off-white crystal **5** under the same condition. Optical characterization with UV−vis and fluorescence spectroscopy was performed for luminescent crystals **1**−**3**. From the UV−vis spectrum of **1** (Figure 1a), the absorption (solids dispersed in $BaSO_4$) spanning from 200 to 520 nm presents a striking contrast vs solution data, which shows major absorption around 200−350 nm. Because carbazole is easily oxidized and

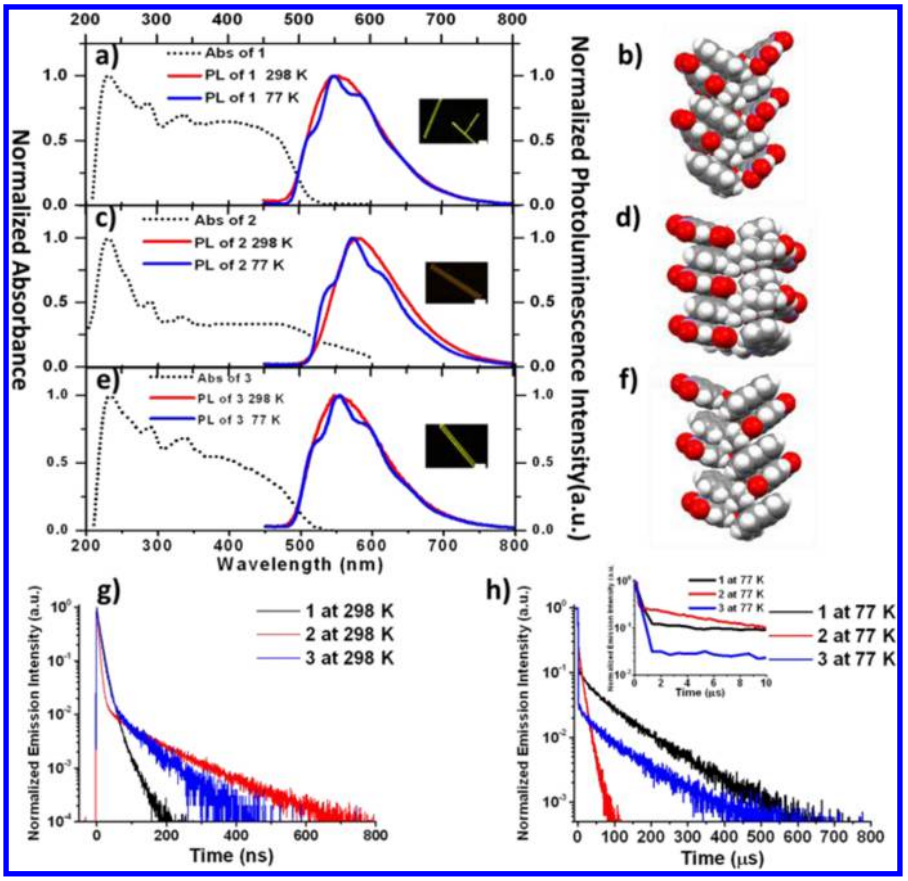

Figure 1. Absorption and steady-state emission spectra (at 298 and 77 K) of FQD CZ-2C-DNB (**1**) (a), CZ-6C-DNB (**2**) (c), and CZ-2C-MNB (**3**) (e) crystals (left *y*-axes for absorption spectrum and right *y*-axes for emission spectrum). Insets: micrographs showing fluorescent single crystals of **1**, **2**, and **3** under UV blue light excitation (scar bar: 200 μm). Space-filling model showing intermolecular stacking of **1** (b), **2** (d), and **3** (f) derived from single-crystal XRD data. Photoluminescence lifetime decays (at λ_{em} max; λ_{ex} = 369 nm) of crystals **1**−**3** at 298 K (g) and 77 K (h). Inset of (h): photoluminescence decay in the first 10 μs showing a fast component and a slow one at 77 K. Because all of the decays are complex (triple exponentials), lifetimes are reported as preexponential weight lifetimes.

DOI: 10.1021/acs.jpca.5b06906
J. Phys. Chem. A XXXX, XXX, XXX−XXX

dinitrobenzoate easily reduced, an intermolecular CT transition seems a plausible interpretation for the new band. The emission of the solid **1**, CZ-2C-DNB, at room temperature (λ_{em} = 548 nm) exhibits an absolute quantum yield (Φ_F) of 1.1%. The measured emission lifetime of **1** is 13.75 ns; as a result, the estimated intrinsic luminescence decay[49] of **1** is 1.26 μs (Table 1).

Table 1. Solid-State Luminescence Properties of FQDs 1−3 at 298 K

	λ_{lim} (nm)[a]	λ_{em} (nm)[b]	Φ_{PL} (%)[c]	τ (ns)[d]	τ_0 (μs)[e]
1	520	548	1.1	13.8	1.3
2	600	583	0.17	30.5	18
3	520	545	0.56	18.0	3.2

[a]Upper wavelength limit in the solid absorption. [b]Photoluminescence emission maximum (λ_{ex} = 385 nm). [c]Absolute quantum yield. [d]Apparent pre-exponential weight-averaged lifetime at emission maximum (excitation: 369 nm diode laser). [e]Estimated intrinsic lifetime at emission maximum all three FQDs ($\tau_0 \sim \tau/\Phi_{PL}$).

The influence of linker length and fluorophore/quencher variation on crystal packing and photoluminescence (PL) has also been explored (Figure 1b−f). When the alkyl linker length is increased by two carbons to six, the PL of **2** solid, CZ-6C-DNB, is red-shifted to 583 nm. For mononitro-substituted quencher, the PL of **3** solid, CZ-2C-MNB, is slightly blue-shifted to 545 nm. The intrinsic lifetimes of solids **2** (17.9 μs) and **3** (3.22 μs) are also within the microsecond domain. The emission spectra of FQD solids **1**−**3** at 77 K were also recorded: they are almost superimposable with those at 298 K except for more defined vibrational structures. When monitored at the same emission maximum for each FQD at 77 K, the measured luminescence lifetimes are consistently much longer (Figure 1h; 115, 13, and 102 μs) compared to those at 298 K (13.8, 30.5, and 18.0 ns), probably owing to diminished thermal decay. When the carbazole fluorophore is changed to fluorene, however (**4** and **5** in Chart 1), the absorption spectra significantly lack transitions in the red region vs carbazole (Figure S2) and no PL could be detected for either solid **4** or **5** under the same experimental conditions. Single-crystal XRD measurements were also performed for FQDs **1**−**5** (Figures 1 and S3). Emissive FQDs **1**−**3** adopt very tight packing, as illustrated by the space-fill presentation (Figure 1b,d,f) from multiple modes of short contacts (Figure S4), which are largely absent in single crystals **4** and **5**. Furthermore, any minor chemical alternation in the dyad (donor, linker, and acceptor) can result in a conspicuous crystal packing change, such as the stacking of aromatic rings and the dihedral angle between the fluorophore and the quencher planes (e.g., a shorter linkage causes a smaller dihedral angle).

To prove that the emissions from solids **1**−**3** are indeed caused by aggregation, we examined the PL of FQD **3** (which has the best solubility) in 2-methyltetrahydrofuran (mTHF) at room temperature; no emission could be detected at all, as expected. At 77 K, mTHF formed a rigid glass and concentration-dependent PL could be observed (Figure S5a). At 10^{-5} M, only faint blue fluorescence characteristic of carbazole was observed (~370 nm, τ = 7.5 ns); at 10^{-2} M, however, yellow and long-lived luminescence (~530 nm, τ = 9.74 μs) (Figure S5b) similar to that of the solid was observed, presumably due to molecular aggregation at a much higher concentration. The excitation spectrum also indicates electronic transitions are much more extended into the lower energy region compared to that in solution (Figure S5c). The absence of a mid-visible (~550 nm) luminescence for any of the FQDs in dilute room-temperature solutions or in 77 K mTHF glasses rules out that the emission arises from discrete FQDs or their components. On the basis of the spectroscopic data, molecular aggregation should be responsible for the observed PL in the solid state for FQDs **1**−**3**. Moreover, we found that none of the amorphous solid samples of **1**−**5** via rapid solvent evaporation exhibits emission, which suggests that the presence of order is also required in the AIE system. Tang et al.[50] recently reported a pure oxygenic nonconjugated polymer and found that the PL origin was due to the clustering of locked carbonyl groups. Compared to our current study, it is possible that the clustering-induced PL is a general feature of many solid-state systems.

A model describing our luminescence and lifetime data is as follows. The emissions all arise from a near degenerate CT singlet triplet pair. The emission probably comes predominantly from the singlet and is thus a delayed fluorescence. In the lifetime measurements, the fast decay is a prompt fluorescence either from a nonequilibrated singlet state or from the lowest singlet state. The long-lived component arises from the thermally equilibrated singlet and triplet states and is largely a delayed fluorescence. At low temperature the lifetime is long because of the lower population of the singlet state relative to the triplet. In this model, the reciprocal of the "intrinsic lifetime" is actually the concentrated weighted rates for the two equilibrated levels. Because at lower temperatures the lower level is more populated, the intrinsic lifetime at low temperatures can be substantially longer than the intrinsic lifetime at room temperature.

To shed more light on the AIE mechanism, we carried out detailed calculations using extracted geometries for single FQDs and FQD clusters. To characterize excitation energies, we used the linear response time-dependent density functional theory (TDDFT)[51−53] with the Head-Gordon functional wB97XD[54,55] and the Dunning cc-pVDZ basis set.[56] The medium was taken to be dichloromethane as represented by the Tomasi continuum model[57] as implemented in Gaussian 09 software.[58] To judge the performance of our models, we compared computed spectra (Figure S6) for *N*-ethylcarbazole, mononitrobenzene, *m*-dinitrobenzene, and 9-methylfluorene in dichloromethane medium with published spectra.[59] We then computed absorption spectra for discrete FQDs **1**−**5** in dichloromethane (represented by the PCM model for the solvent). Experimental spectra (Figure S1) and computed spectra (Figure S7) match up closely, except for a systematic shift of ~0.5 eV. We observed this shift in our calibration calculations on carbazole, fluorene, and the monomeric FQDs. From the calculations, very weak intramolecular CT transitions can be noted for all the FQD monomer (Figure S7). We then calculated the transitions for the FQD clusters (Figure 2), which are responsible for the observed AIE. When two or more FQDs are in close association, intermolecular CT from closely stacked fluorophore−quencher pairs is feasible. We extracted an *N*-methylcarbazole and an ideally associated 3,5-dinitrobenzoate from the crystal structure of CZ-6C-DNB (**2**). When the fluorophore and quencher were coplanar and separated by 3.5 Å, a value closely matching single-crystal data, significant new features of the spectrum corresponding to CT emerged. These features disappeared when the separation was increased to 7.0 Å (Figure 2a), which indicates that the transitions are indeed

DOI: 10.1021/acs.jpca.5b06906
J. Phys. Chem. A XXXX, XXX, XXX−XXX

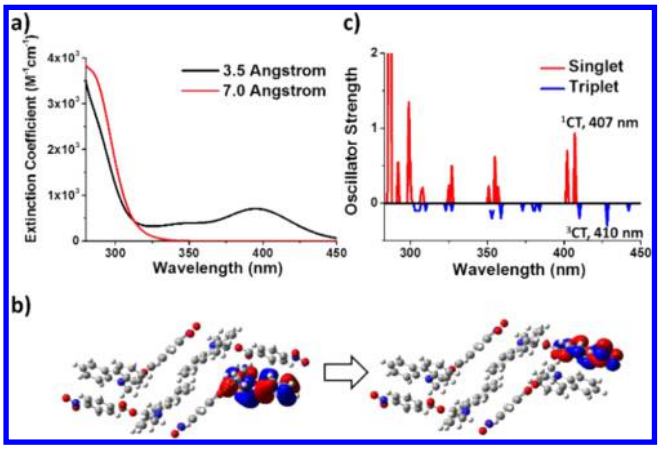

Figure 2. (a) Calculated absorption spectra of stacked fluorophore (carbazole) and quencher (dinitrobenzoate) dimers using coordinates extracted from single-crystal data of CZ-6C-DNB (**2**). Fluorophore and quencher are separated by 3.5 Å (black line) and 7.0 Å (red line) from calculations. (b) Calculated representative charge-transfer transition illustrated with origin and destination orbitals for crystal CZ-2C-MNB (**3**) calculated by the ZINDO model. (c) Oscillator strength f (×100) vs wavelength for the CZ-6C-DNB model stacked by 3.5 Å showing both singlet and triplet transitions. The orbitals derive from the wB97XD/cc-pVDZ (PCM dichloromethane) calculation on a dimer with geometry from the crystal, as extracted by MERCURY.

from intermolecular CT states. The packing for the CZ-6C-DNB FQD allows ideal stacking; in the dimer of dyads, every donor has an acceptor nearby, and the alignment is nearly perfect. In the CZ-6C-DNB FQD dimer extracted from the crystal geometry we see almost exactly the same spectrum as is displayed in the untethered model. Calculations on FQD tetramers produced spectra very similar to the spectra calculation for dyad dimers and confirmed that charge transfer occurs between near neighbors. This is consistent with the computations on untethered stacking models with planar carbazole or fluorene separated from a dinitrobenzoate plane by 3.5 and 7.0 Å. No charge transfer occurs at the greater separation. *Therefore, the excited state is largely localized on one intermolecular carbazole−nitrobenzoate pair.* A representative intermolecular CT transition is given in Figure 2b, where the origin and destination are located in the carbazole and a neighboring dinitrobenzoate molecules, respectively. We did the same calculations for the fluorene FQD systems (**4** and **5**), which are closely analogous to the carbazole ones (**1**−**3**). The subtle differences are important however: although there is both intramolecular CT (to be seen in the FQD monomer) and intermolecular CT (emerging in the dimer), both occur at higher energy and with lower intensity in fluorene FQD systems relative to the carbazole systems. The absence of low-lying intermolecular CT states is consistent with much greater difficulty of oxidizing fluorene than carbazole.[60,61] Although absorption spectra yield information only on the singlet states, triplet states should intimately be involved in the emission spectra: the poor orbital overlap in the intermolecular CT state indicates very small exchange energy and thus rapid intersystem crossing rate. Indeed, calculation results show that the singlet and triplet energy levels for the lowest CT state are almost degenerate in the CZ-6C-DNB dimer (Figure 2c). The near degeneracy of the singlet and triplet CT states slows the decay and extends the calculated radiative and observed lifetimes into the microsecond range. In addition, from Figure 1h, a fast decay component and a much slower one could be readily observed, presumably corresponding to the singlet and triplet decays, respectively. Our work is also consistent with results published by Adachi et al.[62−64] who reported a series of intramolecular CT organic dyes that possess almost degenerate singlet−triplet states when minimal orbital overlap is involved for the origin and destination. The current AIE system, however, presents such an example that intermolecular CT states from isolated electronic systems can also be used to achieve the same goal.

Finally, we noticed, during the course of experiments, that solution-cast samples could occasionally scatter blue light under ambient lighting, which is an indication of nanostructures. After an acetone solution of CZ-2C-DNB (10^{-4} M) was dried in air on a borosilicate substrate, luminescent wires up to a few hundred micrometers were observed under a fluorescence microscope (100×, Figure 3a). Transmission electron micros-

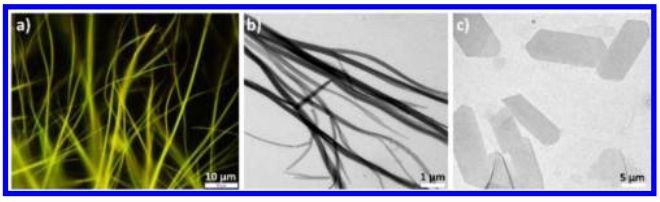

Figure 3. (a) Fluorescence microscopy image of acetone solution-cast **1** on a glass slide (a, λ_{ex} ∼ 420−450 nm). (b) and (c) TEM images of solution cast **1** on copper plates from acetone and methanol.

copy revealed nanowire-like structures (Figure 3b). These nanowires are typically 100−200 μm in length and 200−400 nm in width and are highly reproducible. In methanol, however, in addition to the nanowires, nanosheets were also obtained (Figure 3c). The differences in molecular packing and thermodynamic stability of the two polymorphs warrant further investigation. Nonetheless, such microscopic structures could be important in self-assembly-based nano-optoelectronics.[44]

CONCLUSIONS

In summary, we constructed a new class of AIE-active molecular materials based on fluorophore−quencher dyads (FQDs) and obtained long-lived solid-state luminescence, which is absent in solutions. From spectroscopic measurement, single-crystal data and theoretical calculations, the long-lived emission is ascribed to an intermolecular CT state with nearly degenerate singlet−triplet energy levels. These FQDs could self-assemble into luminescent nanowires and nanosheets under different conditions. This strategy has opened new doors for generating a new class of AIE-active materials based on intermolecular CT. We are currently exploring other fluorophore−linker−quencher systems to investigate the generality of the strategy.

ASSOCIATED CONTENT

Supporting Information

The Supporting Information is available free of charge on the ACS Publications website at DOI: 10.1021/acs.jpca.5b06906.

Materials, methods, syntheses of compounds **1**−**5**, and supplementary figures, including UV absorption of **1**−**5** in dilute solution, solid-state UV absorption and crystal packing of **4** and **5**, multiple modes of short contacts in **1** crystal from single-crystal XRD data, emission spectra of **3** at 77 K, and computed UV absorption of **1**−**5** (PDF)

DOI: 10.1021/acs.jpca.5b06906
J. Phys. Chem. A XXXX, XXX, XXX−XXX

CIF file for $C_{21}H_{15}N_3O_6$ (CIF)
CIF file for $C_{25}H_{23}N_3O_6$ (CIF)
CIF file for $C_{21}H_{16}N_2O_4$ (CIF)
CIF file for $C_{21}H_{14}N_2O_6$ (CIF)
CIF file for $C_{21}H_{15}NO_4$ (CIF)

AUTHOR INFORMATION

Corresponding Author

*G. Zhang. E-mail: gz6m@virginia.edu.

Notes

The authors declare no competing financial interest.

ACKNOWLEDGMENTS

G.Z. thanks the National Natural Science Foundation of China (NSFC) for support of this work (21222405). R.E.E. acknowledges support from the NSF GRFP. C.O.T. is grateful for support for computer equipment and travel from the Body Foundation.

REFERENCES

(1) Zhao, Z.; Lam, J. W.; Tang, B. Z. Tetraphenylethene: a versatile AIE building block for the construction of efficient luminescent materials for organic light-emitting diodes. *J. Mater. Chem.* **2012**, *22*, 23726−23740.

(2) Wang, H.; Zhao, E.; Lam, J. W.; Tang, B. Z. AIE luminogens: emission brightened by aggregation. *Mater. Today* **2015**, DOI: 10.1016/j.mattod.2015.03.004.

(3) Jelley, E. E. Spectral absorption and fluorescence of dyes in the molecular state. *Nature* **1936**, *138*, 1009−1010.

(4) Scheibe, G. Über die veränderlichkeit der absorptionsspektren in lösung und die van der Waalsschen Kräfte als ihre ursache. *Angew. Chem.* **1937**, *50*, 51.

(5) Scheibe, G. On the changeability of the absorption spectrum of dyes in solutions and the aggregation as its cause. *Angew. Chem.* **1937**, *50*, 212−219.

(6) Mei, J.; Hong, Y.; Lam, J. W.; Qin, A.; Tang, Y.; Tang, B. Z. Aggregation-induced emission: the whole is more brilliant than the parts. *Adv. Mater.* **2014**, *26*, 5429−5479.

(7) Huang, J.; Sun, N.; Dong, Y.; Tang, R.; Lu, P.; Cai, P.; Li, Q.; Ma, D.; Qin, J.; Li, Z. Similar or totally different: the control of conjugation degree through minor structural modifications, and deep-blue aggregation-induced emission luminogens for non-doped OLEDs. *Adv. Funct. Mater.* **2013**, *23*, 2329−2337.

(8) Hong, Y.; Lam, J. W.; Tang, B. Z. Aggregation-induced emission. *Chem. Soc. Rev.* **2011**, *40*, 5361−5388.

(9) Klessinger, M.; Michl, J. *Excited states and photochemistry of organic molecules*; VCH: Weinheim, 1995.

(10) Oelkrug, D.; Tompert, A.; Gierschner, J.; Egelhaaf, H.-J.; Hanack, M.; Hohloch, M.; Steinhuber, E. Tuning of fluorescence in films and nanoparticles of oligophenylenevinylenes. *J. Phys. Chem. B* **1998**, *102*, 1902−1907.

(11) Zhang, M.; Feng, G.; Song, Z.; Zhou, Y.-P.; Chao, H.-Y.; Yuan, D.; Tan, T. T.; Guo, Z.; Hu, Z.; Tang, B. Z. Two-dimensional metal−organic framework with wide channels and responsive turn-on fluorescence for the chemical sensing of volatile organic compounds. *J. Am. Chem. Soc.* **2014**, *136*, 7241−7244.

(12) Yuan, W. Z.; Yu, Z.-Q.; Lu, P.; Deng, C.; Lam, J. W.; Wang, Z.; Chen, E.-Q.; Ma, Y.; Tang, B. Z. High efficiency luminescent liquid crystal: aggregation-induced emission strategy and biaxially oriented mesomorphic structure. *J. Mater. Chem.* **2012**, *22*, 3323−3326.

(13) Wang, J.; Mei, J.; Yuan, W.; Lu, P.; Qin, A.; Sun, J.; Ma, Y.; Tang, B. Z. Hyperbranched polytriazoles with high molecular compressibility: aggregation-induced emission and superamplified explosive detection. *J. Mater. Chem.* **2011**, *21*, 4056−4059.

(14) Liu, Y.; Tang, Y.; Barashkov, N. N.; Irgibaeva, I. S.; Lam, J. W.; Hu, R.; Birimzhanova, D.; Yu, Y.; Tang, B. Z. Fluorescent chemosensor for detection and quantitation of carbon dioxide gas. *J. Am. Chem. Soc.* **2010**, *132*, 13951−13953.

(15) Liang, G.; Weng, L.-T.; Lam, J. W.; Qin, W.; Tang, B. Z. Crystallization-induced hybrid nano-sheets of fluorescent polymers with aggregation-induced emission characteristics for sensitive explosive detection. *ACS Macro Lett.* **2013**, *3*, 21−25.

(16) Zhang, X.; Zhang, X.; Tao, L.; Chi, Z.; Xu, J.; Wei, Y. Aggregation induced emission-based fluorescent nanoparticles: fabrication methodologies and biomedical applications. *J. Mater. Chem. B* **2014**, *2*, 4398−4414.

(17) Yuan, Y.; Zhang, C. J.; Gao, M.; Zhang, R.; Tang, B. Z.; Liu, B. Specific light-up bioprobe with aggregation-induced emission and activatable photoactivity for the targeted and image-guided photodynamic ablation of cancer cells. *Angew. Chem., Int. Ed.* **2015**, *54*, 1780−1786.

(18) Wang, D.; Qian, J.; Qin, W.; Qin, A.; Tang, B. Z.; He, S. Biocompatible and photostable AIE dots with red emission for in vivo two-photon bioimaging. *Sci. Rep.* **2014**, *4*, 4279.

(19) Liang, J.; Tang, B. Z.; Liu, B. Specific light-up bioprobes based on AIEgen conjugates. *Chem. Soc. Rev.* **2015**, *44*, 2798−2811.

(20) Leung, C. W. T.; Hong, Y.; Chen, S.; Zhao, E.; Lam, J. W. Y.; Tang, B. Z. A photostable AIE luminogen for specific mitochondrial imaging and tracking. *J. Am. Chem. Soc.* **2013**, *135*, 62−65.

(21) Geng, J.; Li, K.; Ding, D.; Zhang, X.; Qin, W.; Liu, J.; Tang, B. Z.; Liu, B. Lipid-PEG-folate encapsulated nanoparticles with aggregation induced emission characteristics: cellular uptake mechanism and two-photon fluorescence imaging. *Small* **2012**, *8*, 3655−3663.

(22) Ding, D.; Li, K.; Liu, B.; Tang, B. Z. Bioprobes based on AIE fluorogens. *Acc. Chem. Res.* **2013**, *46*, 2441−2453.

(23) Ding, D.; Goh, C. C.; Feng, G.; Zhao, Z.; Liu, J.; Liu, R.; Tomczak, N.; Geng, J.; Tang, B. Z.; Ng, L. G. Ultrabright organic dots with aggregation-induced emission characteristics for real-time two-photon intravital vasculature imaging. *Adv. Mater.* **2013**, *25*, 6083−6088.

(24) Peng, Q.; Yi, Y.; Shuai, Z.; Shao, J. Toward quantitative prediction of molecular fluorescence quantum efficiency: role of Duschinsky rotation. *J. Am. Chem. Soc.* **2007**, *129*, 9333−9339.

(25) Li, S.; Wang, Q.; Qian, Y.; Wang, S.; Li, Y.; Yang, G. Understanding the pressure-induced emission enhancement for triple fluorescent compound with excited-state intramolecular proton transfer. *J. Phys. Chem. A* **2007**, *111*, 11793−11800.

(26) Chen, J.; Law, C. C.; Lam, J. W.; Dong, Y.; Lo, S. M.; Williams, I. D.; Zhu, D.; Tang, B. Z. Synthesis, light emission, nanoaggregation, and restricted intramolecular rotation of 1, 1-substituted 2, 3, 4, 5-tetraphenylsiloles. *Chem. Mater.* **2003**, *15*, 1535−1546.

(27) Zhang, G.-F.; Aldred, M. P.; Gong, W.-L.; Li, C.; Zhu, M.-Q. Utilising tetraphenylethene as a dual activator for intramolecular charge transfer and aggregation induced emission. *Chem. Commun.* **2012**, *48*, 7711−7713.

(28) Yang, Z.; Qin, W.; Lam, J. W.; Chen, S.; Sung, H. H.; Williams, I. D.; Tang, B. Z. Fluorescent pH sensor constructed from a heteroatom-containing luminogen with tunable AIE and ICT characteristics. *Chem. Sci.* **2013**, *4*, 3725−3730.

(29) Gong, Y.; Zhang, Y.; Yuan, W. Z.; Sun, J. Z.; Zhang, Y. D−A solid emitter with crowded and remarkably twisted conformations exhibiting multifunctionality and multicolor mechanochromism. *J. Phys. Chem. C* **2014**, *118*, 10998−11005.

(30) Gong, Y.; Tan, Y.; Liu, J.; Lu, P.; Feng, C.; Yuan, W. Z.; Lu, Y.; Sun, J. Z.; He, G.; Zhang, Y. Twisted D−π−A solid emitters: efficient emission and high contrast mechanochromism. *Chem. Commun.* **2013**, *49*, 4009−4011.

(31) Yuan, H.; Wang, K.; Yang, K.; Liu, B.; Zou, B. Luminescence properties of compressed tetraphenylethene: the role of intermolecular interactions. *J. Phys. Chem. Lett.* **2014**, *5*, 2968−2973.

(32) Roy, S.; Stollberg, P.; Herbst-Irmer, R.; Stalke, D.; Andrada, D. M.; Frenking, G.; Roesky, H. W. Carbene-dichlorosilylene stabilized phosphinidenes exhibiting strong intramolecular charge transfer transition. *J. Am. Chem. Soc.* **2015**, *137*, 150−153.

DOI: 10.1021/acs.jpca.5b06906
J. Phys. Chem. A XXXX, XXX, XXX−XXX

(33) Courtney, T. L.; Fox, Z. W.; Estergreen, L.; Khalil, M. Measuring coherently coupled intramolecular vibrational and charge-transfer dynamics with two-dimensional vibrational−electronic spectroscopy. *J. Phys. Chem. Lett.* **2015**, *6*, 1286−1292.
(34) Meng, X.; Qi, G.; Zhang, C.; Wang, K.; Zou, B.; Ma, Y. Visible mechanochromic responses of spiropyrans in crystals via pressure-induced isomerization. *Chem. Commun.* **2015**, *51*, 9320−9323.
(35) Perveaux, A.; Castro, P. J.; Lauvergnat, D.; Reguero, M.; Lasorne, B. Intramolecular charge transfer in 4-aminobenzonitrile does not need the twist and may not need the bend. *J. Phys. Chem. Lett.* **2015**, *6*, 1316−1320.
(36) Wang, Y.; Tan, X.; Zhang, Y.-M.; Zhu, S.; Zhang, I.; Yu, B.; Wang, K.; Yang, B.; Li, M.; Zou, B. Dynamic behavior of molecular switches in crystal under pressure and its reflection on tactile sensing. *J. Am. Chem. Soc.* **2015**, *137*, 931−939.
(37) Zhang, Y.; Wang, K.; Zhuang, G.; Xie, Z.; Zhang, C.; Cao, F.; Pan, G.; Chen, H.; Zou, B.; Ma, Y. Multicolored-fluorescence switching of ICT-type organic solids with clear color difference: mechanically controlled excited state. *Chem. - Eur. J.* **2015**, *21*, 2474−2479.
(38) Yang, J.-S.; Swager, T. M. Porous shape persistent fluorescent polymer films: an approach to TNT sensory materials. *J. Am. Chem. Soc.* **1998**, *120*, 5321−5322.
(39) Myers, A. B. Resonance Raman intensities and charge-transfer reorganization energies. *Chem. Rev.* **1996**, *96*, 911−926.
(40) Swamy, K. M. K.; Ko, S.-K.; et al. Boronic acid-linked fluorescent and colorimetric probes for copper ions. *Chem. Commun.* **2008**, 5915−5917.
(41) Germain, M. E.; Knapp, M. J. Optical explosives detection: from color changes to fluorescence turn-on. *Chem. Soc. Rev.* **2009**, *38*, 2543−2555.
(42) Gabe, Y.; Urano, Y.; Kikuchi, K.; Kojima, H.; Nagano, T. Highly sensitive fluorescence probes for nitric oxide based on boron dipyrromethene chromophore rational design of potentially useful bioimaging fluorescence probe. *J. Am. Chem. Soc.* **2004**, *126*, 3357−3367.
(43) De Silva, A. P.; Gunaratne, H. N.; Gunnlaugsson, T.; Huxley, A. J.; McCoy, C. P.; Rademacher, J. T.; Rice, T. E. Signaling recognition events with fluorescent sensors and switches. *Chem. Rev.* **1997**, *97*, 1515−1566.
(44) Das, A.; Ghosh, S. Supramolecular assemblies by charge-transfer interactions between donor and acceptor chromophores. *Angew. Chem., Int. Ed.* **2014**, *53*, 2038−2054.
(45) Beddard, G.; Carlin, S.; Harris, L.; Porter, G.; Tredwell, C. Quenching of chlorophyll fluorescence by nitrobenzene. *Photochem. Photobiol.* **1978**, *27*, 433−438.
(46) Park, S. K.; Varghese, S.; Kim, J. H.; Yoon, S.-J.; Kwon, O. K.; An, B.-K.; Gierschner, J.; Park, S. Y. Tailor-made highly luminescent and ambipolar transporting organic mixed stacked charge-transfer crystals: an isometric donor−acceptor approach. *J. Am. Chem. Soc.* **2013**, *135*, 4757−4764.
(47) Masuo, S.; Yamane, Y.; Machida, S.; Itaya, A. Fluorescence behavior of individual charge-transfer complexes revealed by single-molecule fluorescence spectroscopy: influence of the host polymer matrix. *J. Photochem. Photobiol., A* **2012**, *227*, 65−70.
(48) Kwon, M. S.; Gierschner, J.; Yoon, S. J.; Park, S. Y. Unique piezochromic fluorescence behavior of dicyanodistyrylbenzene based donor−acceptor−donor triad: mechanically controlled photo-induced electron transfer (eT) in molecular assemblies. *Adv. Mater.* **2012**, *24*, 5487−5492.
(49) Lakowicz, J. R. *Principles of fluorescence spectroscopy*; Springer Science & Business Media: Berlin, 2013.
(50) Zhao, E.; Lam, J. W.; Meng, L.; Hong, Y.; Deng, H.; Bai, G.; Huang, X.; Hao, J.; Tang, B. Z. Poly [(maleic anhydride)-alt-(vinyl acetate)]: a pure oxygenic nonconjugated macromolecule with strong light emission and solvatochromic effect. *Macromolecules* **2015**, *48*, 64−71.
(51) Runge, E.; Gross, E K U. Density-functional theory for time-dependent systems. *Phys. Rev. Lett.* **1984**, *52*, 997.
(52) Bauernschmitt, R.; Ahlrichs, R. Treatment of electronic excitations within the adiabatic approximation of time dependent density functional theory. *Chem. Phys. Lett.* **1996**, *256*, 454−464.
(53) Stratmann, R. E.; Scuseria, G. E.; Frisch, M. J. An efficient implementation of time-dependent density-functional theory for the calculation of excitation energies of large molecules. *J. Chem. Phys.* **1998**, *109*, 8218−8224.
(54) Chai, J. D.; Head-Gordon, M. Systematic optimization of long-range corrected hybrid density functionals. *J. Chem. Phys.* **2008**, *128*, 084106.
(55) Chai, J. D.; Head-Gordon, M. Long-range corrected hybrid density functionals with damped atom−atom dispersion corrections. *Phys. Chem. Chem. Phys.* **2008**, *10*, 6615−6620.
(56) Dunning, T. H., Jr Gaussian basis sets for use in correlated molecular calculations. I. The atoms boron through neon and hydrogen. *J. Chem. Phys.* **1989**, *90*, 1007−1023.
(57) Tomasi, J.; Mennucci, B.; Cammi, R. Quantum mechanical continuum solvation models. *Chem. Rev.* **2005**, *105*, 2999−3094.
(58) Frisch, M. J.; Trucks, G. W.; Schlegel, H. B.; et al. *Gaussian 09*, Revision D.01; Gaussian. Inc.: Wallingford, CT, 2009.
(59) Linstrom, P.; Mallard, W. *NIST Chemistry WebBook*; NIST standard reference database No. 69; National Institute of Standards and Technology: Gaithersburg, MD, 2001.
(60) Majcherczyk, A.; Johannes, C.; Hüttermann, A. Oxidation of polycyclic aromatic hydrocarbons (PAH) by laccase of trametes versicolor. *Enzyme Microb. Technol.* **1998**, *22*, 335−341.
(61) Ambrose, J.; Nelson, R. Anodic oxidation pathways of carbazoles I. carbazole and N-substituted derivatives. *J. Electrochem. Soc.* **1968**, *115*, 1159−1164.
(62) Zhang, Q.; Li, B.; Huang, S.; Nomura, H.; Tanaka, H.; Adachi, C. Efficient blue organic light-emitting diodes employing thermally activated delayed fluorescence. *Nat. Photonics* **2014**, *8*, 326−332.
(63) Uoyama, H.; Goushi, K.; Shizu, K.; Nomura, H.; Adachi, C. Highly efficient organic light-emitting diodes from delayed fluorescence. *Nature* **2012**, *492*, 234−238.
(64) Sato, K.; Shizu, K.; Yoshimura, K.; Kawada, A.; Miyazaki, H.; Adachi, C. Organic luminescent molecule with energetically equivalent singlet and triplet excited states for organic light-emitting diodes. *Phys. Rev. Lett.* **2013**, *110*, 247401.

DOI: 10.1021/acs.jpca.5b06906
J. Phys. Chem. A XXXX, XXX, XXX−XXX